An investigation into the origin of aerosol nucleation events observed in the Southern Ocean boundary layer

S.I. Jimi[1,2], S.T. Siems[2,3], J.L. McGregor[4], J.L. Gras[4] and J.J. Katzfey[4]
[1]School of Geography and Environmental Science, Monash University, Australia
[2]Climate Theme, Monash Sustainability Institute, Monash University, Australia
[3]School of Mathematical Sciences, Monash University, Australia
[4]CSIRO Marine and Atmospheric Research, Australia

(Manuscript submitted May 2007; revised February 2008)

A clear picture of the physical processes involved in the nucleation of aerosol particles in the boundary layer (BL) over the remote Southern Ocean remains elusive due to the lack of definitive observations. A month-long observation aboard a ship during the first aerosol characterisation experiment (ACE-1) suggested that some enhanced aerosol nucleation events were linked to the passage of a frontal system. However, the cause of the link between frontal passages and nucleation events could not be determined from a statistical analysis of two years of surface observations at the Cape Grim Baseline Air Pollution Station (CGBAPS). In this paper, numerical simulations are combined with satellite imagery, synoptic analysis and surface observations at CGBAPS to further investigate the origin of observed nucleation events during the passage of a frontal system. This analysis suggests that nanoparticles are formed at or just above the BL inversion by relatively common shallow post-frontal cumulus clouds. The BL then entrains these new particles in a process that helps maintain the overall aerosol population.

Introduction

Aerosol nucleation events are typically identified by the simple observation of elevated concentrations of nanoparticles or ultrafine particles defined here as particles with a diameter (Dp) in the range 3 to 12 nm determined using two condensation particle counters, a TSI 3025 UCPC (Dp ≥ 3 nm) and a TSI CN3760 (Dp ≥ 12 nm). Such events, as the name would suggest, are episodic in nature with the particles formed by specific meteorological and environmental processes that lead to levels of precursor gases required for particle nucleation. Some specific cases, where new particle production is evident, have been observed previously in the remote marine boundary layer (BL), including enhancement of nanoparticle concentrations during events associated with frontal passages or subsidence (Hogan and Barnard 1978; Covert et al. 1996). Sporadic nanoparticle events in the marine BL were also observed following the removal of existing particles by precipitation and the subsequent reduction of aerosol surface area (Covert et al. 1992). Strong coastal production of particles is frequently observed during low tide and a strong solar irradiation (O'Dowd et al. 1998, 2002).

Corresponding author address: Salah I. Jimi, School of Geography and Environmental Science, Monash University, Monash, Vic. 3800, Australia.
Email: Salah.Jimi@arts.monash.edu.au

Aerosol nucleation events in the free troposphere (FT) in the vicinity of clouds are commonly observed. For example, Clarke et al. (1998) observed elevated nanoparticle concentrations in the upper FT over the Southern Ocean during the First Aerosol Characterization Experiment (ACE-1). These *in situ* aircraft observations were readily traced back to their origin in the detrained air from deep convection, which was rich in sulfates originally available in the BL. In the absence of existing particles in the FT on which the precursor gases could condense, the sulfate nucleated into nanoparticles. Similarly, during ACE-1, Weber et al. (2001) observed nanoparticles in the upper FT when flying near a frontal system. It was suggested that the nucleation was in response to the anvil outflow of the frontal system and also depended on the observed strong actinic flux at the top of the frontal clouds. In both instances, physical processes believed to be responsible for the aerosol formation were identified.

However, observations of nucleation events in the BL (Bates et al. 1998) aboard a ship in the remote Southern Ocean have proven more difficult to fully explain. In theory, it should be difficult to create new particles in the remote maritime BL (e.g. Bigg et al. 1984; Ito 1985; Clarke 1993; Raes 1995). Any excess gas molecules would preferentially condense on pre-existing aerosols rather than undergoing nucleation; the existing aerosol surface area in the BL is too large to afford new particle formation via gas-to-particle conversion (GPC) (Cainey and Harvey 2002).

While entrained air from the FT could bring down submicron particles into the BL as reported by Raes (1995), it is difficult to imagine that the nanoparticles investigated in this study would have formed in the upper FT. The nanoparticles observed by Clarke et al. (1998) and Weber et al. (2001) should take days to subside down to the BL inversion. It is easily shown that for Southern Ocean conditions the coagulation lifetime of nanoparticles is of the order of hours only. Thus it would appear that these upper troposphere nucleation events are not directly related to the BL observations of Bates et al. (1998).

Rapid downdrafts through the FT are possible in the immediate neighborhood of deep convection and frontal passages. Indeed, Bates et al. (1998) linked the source of the observed BL nucleation events to the passage of the mid-latitude cold fronts that are prevalent over the Southern Ocean. Frontal passages are the dominant meteorological phenomenon in the mid-latitudes and can occur with a frequency of four to eight days during the late spring, as was the case during ACE-1. These nucleation events, however, were observed to follow the passage of a cold front by a matter of six to 24 hours or hundreds of kilometres. It is not immediately apparent that these surface observations occur directly in relation to the frontal passage or any deep convection.

Jimi (2004) analysed two years of data of nucleation events as observed at the Cape Grim Baseline Air Pollution Station (CGBAPS), giving a detailed description of the nucleation events and a statistical analysis of the relationship between these nucleation events and the preceding frontal passage. Jimi found no meaningful correlation between the characteristics of the nucleation event and those of the frontal passage, but showed that the nucleation events were weakly correlated with the post-frontal BL air mass as defined by its wind speed and water vapour content.

In this paper, the meteorological history of these nucleation events is explored indirectly through broader synoptic observations and numerical simulations. We first review the dominant meteorology and its relation to the observed nucleation events. Six case studies have been examined in an effort to identify a potential mechanism for the observed nucleation events. Given the limited ability of fixed surface observations to identify the source of these nucleation events, the regional meteorology of these case studies has been simulated with a mesoscale meteorological model. These simulations are explored to gain insight into the dynamics of the marine BL that may have led to the entrainment of the nanoparticles and the observed nucleation events. Also, ozone is employed as a marker of FT air, since its concentration in the troposphere is, on average, greater than in the BL and the variance between the two concentrations can be used to indicate entrainment of air from aloft.

Meteorology of a nucleation event

In the lower FT, the meteorology over much of the Southern Ocean is dominated by baroclinic instabilities, where subpolar air masses mix with subtropical air masses in a series of frontal passages. The cold subpolar air mass which arrives from the southwest to west is commonly free of any short-term (days to weeks) anthropogenic influence. It is during these baseline conditions that nucleation events are observed at CGBAPS. During the years of 1999 and 2000, Jimi (2004) examined the meteorological records at the CGBAPS and identified 116 such frontal passages. Of these, 84 fronts were observed to give way to a sustained post-frontal period in which baseline air reached CGBAPS. Of these 84 post-frontal periods, 79 were observed to have nucleation events embedded within them.

As a winter example, Fig. 1 shows the mean sea-level pressure (MSLP) charts at 0000 UTC (Coordinated Universal Time) on 14 and 15 August 2000. A front is located to the west of CGBAPS (40° 41′S, 144° 41′E) on 14 August with the heart of the mid-latitude cyclone to the south. The cold front was

Fig. 1 MSLP at 0000 UTC for 14 and 15 August 2000 (courtesy of Australian Bureau of Meteorology).

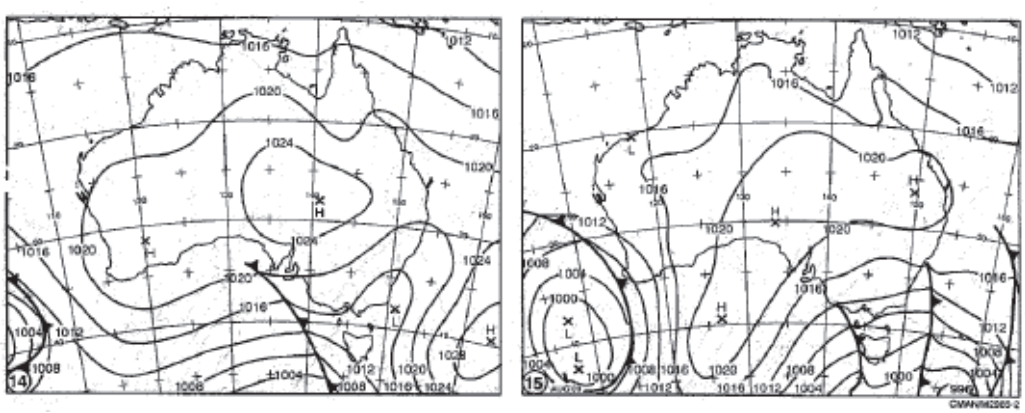

recorded to pass CGBAPS near 0500 UTC on the same day. The pre-frontal air mass is seen to be coming from the northwest, and as the cold front passes over, the winds rapidly swing around to the southwest. Over the 24 hours following this cold front, a subpolar air mass is observed at CGBAPS.

In the first hours immediately following this frontal passage, the CGBAPS observations indicated relatively clean air with minimal concentrations of nanoparticles. An aerosol nucleation event was observed to begin at 1700 UTC and persist for 12 hours (Fig. 2). The peak concentration (450 cm^{-3}) for this event was observed at 2300 UTC, 18 hours after the frontal passage was observed.

The infrared satellite imagery (GMS IR) for 0032 UTC 14 August 2000 (Fig. 3) reveals the approximate location of the front by the positioning of a band of heavy clouds running from the northwest to southeast. Immediately to the west of the front, a band of cloud-free air is observed. Following this band of cloud-free air, a region of shallow, low-level cumulus clouds is observed by the IR imagery. Moving forward to the peak of the nucleation event (2300 UTC), we will see this cloud regime to be prevalent in the vicinity of CGBAPS. All satellite photos for the six cases investigated show these shallow clouds. Figure 4 displays a National Oceanic and Atmospheric Administration Advanced Very High Resolution Radiometer (NOAA AVHRR) visible image around 0800 UTC 14 August 2000; this high resolution image further illustrates the nature of the shallow cumulus clouds.

The observation of such clouds is quite common in this context of a post-frontal air mass. The Southern Ocean Cloud Experiment (SOCEX I and II, Boers et al. (1994)) examined such cloud structures with respect to their radiative properties and cloud micro-

Fig. 2 Surface pressure and nanoparticle concentration observed at the Cape Grim Baseline air pollution station for 14 through to mid 16 August 2000.

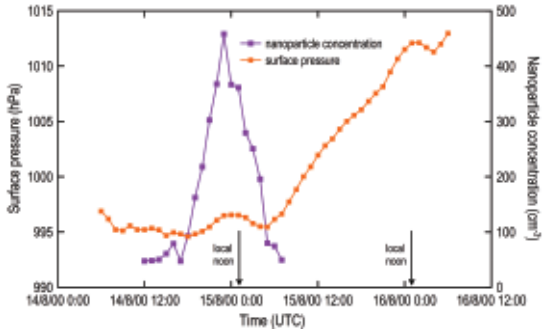

Fig. 3 GMS IR satellite imagery at 0032 UTC for 14 August 2000 (courtesy of Australian Bureau of Meteorology).

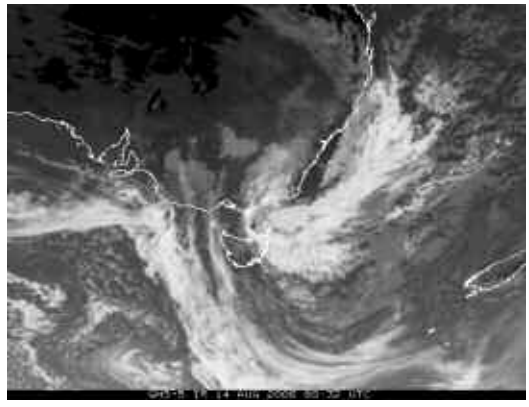

Fig. 4 NOAA AVHRR visible image for 14 August 2000.

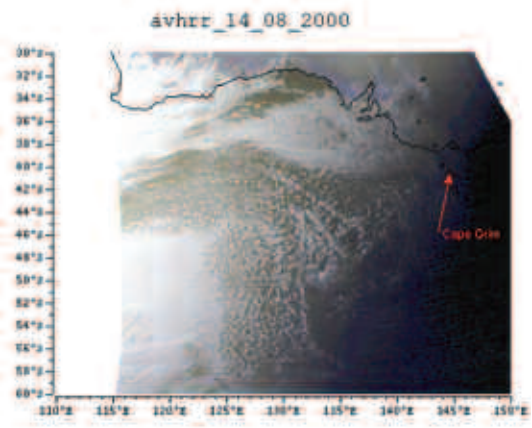

physics. These shallow cumulus clouds commonly fill out and even evolve into a stratocumulus further from the front. This stratocumulus deck is associated with a surface high pressure ridge commonly observed between any two fronts. Beyond this region of post-frontal, anticyclonic BL clouds, a build-up towards the next frontal passage is observed. Unfortunately we have no direct *in situ* nanoparticle observations of these shallow, post-frontal cumuli. The BL flights made during ACE-1, for example, specifically focussed on cloud-free regions.

Seeking to further explore this hypothesis, we consider the BL dynamics at the time of the observed nucleation events. If these shallow cumuli were to be the source, then we would expect to find a well-defined BL and strong entrainment down into the BL from the cumulus while these events build. The CGBAPS measurements do not directly observe the depth of the BL or its entrainment rate. In general, as the marine BL entrains air, it mixes in dry free tropospheric air, so processes such as deepening of the BL and entrainment rate hypothesised to be responsible for the enhanced nanoparticle events in the BL reported here can be inferred from the surface observations.

In an effort to explore more fully the relationship between the meteorology and the observed nucleation events, Table 1 details six of the 79 nucleation events observed by Jimi (2004): four summertime and two wintertime events. A detailed synoptic analysis has been undertaken for these six additional case studies. For all of these cases, satellite imagery shows that low-level cumuli were present at the time of the nucleation events. This basic meteorology is similar during the summer, except that the frontal structure is normally shifted poleward, making it more common for these frontal systems to slip too far to the south to be observed at CGBAPS.

Table 1 defines the changes in water vapour content and temperature in the BL over the course of a nucleation event for these six case studies. These calculated changes were based on the difference between the immediate three-hour post-frontal average and the average during the nanoparticle enhancement period. The observed decreases in water vapour mixing ratio and temperature were typically around 0.6–3.7 g kg^{-1} and 0.3–1.5K, respectively. The data in Table 1 suggest that the thermodynamic measurements at CGBAPS are consistent with a period of time in which the BL would be entraining air from the FT. For the six cases considered, the BL is observed to be drying and cooling during the time of the nucleation event. We note that the change in wind speed is not necessarily a good proxy for entrainment. While the overlying FT would normally have greater wind speeds than the BL, this is not necessarily the case when the region is under a high or ridge. Moreover, the surface winds are generally observed to be greatest at the time of frontal passages.

Table 1. Observed nucleation events and associated surface meteorology observed at Cape Grim.

Time of nucleation event peak (UTC)	*Time lag from preceding front (hours)*	*Duration of event (hours)*	*Δ BL water vapour*	*Δ BL temperature (K)*
0300 15 Feb 1999	9	25	11.8-8.1	289.9-289.5
1700 17 Feb 1999	18	36	10.1-6.8	287.7-286.5
2300 03 Jun 2000	5	13	5.8-5.2	282.8-282.7
2300 14 Aug 2000	18	12.5	7.0-4.3	283.5-281.9
0000 12 Dec 2000	30	12	10.8-8.7	289.6-289.3
0000 18 Dec 2000	17	15	11.7-8.1	290.4-289.6

Numerical simulations

In the absence of any direct observation of entrainment rate at the time of the post-frontal, shallow cumuli, numerical simulations of the six case studies from Table 1 have been undertaken. This numerical investigation of the meteorology also allows for numerical back-trajectories to be created, providing further insight into the history of the air masses that experience these nucleation events. The numerical model employed for these simulations does not include aerosols. Any connection between an enhanced entrainment rate and the observation of a nucleation event at the surface is inferred.

The cubic-conformal atmospheric model (C-CAM) is a two time-level, semi-implicit, hydrostatic, primitive equations model with a semi-Lagrangian horizontal advection scheme on a conformal-cubic grid (McGregor 1996; McGregor and Dix 2001). This model makes a conformal map of the globe onto a cubic surface, with each of the six sides of the cube covered with a 48 by 48 grid. This conformal map, however, is stretched to allow for a much finer resolution over Australia than the far side of the globe; Australia is covered at a resolution of approximately 0.5° (or 60 km). In the vertical, the model runs on normalised pressure, sigma coordinates, defined by the ratio of actual pressure to the surface pressure of approximately 1000 hPa. These simulations have 18 levels in the vertical with nine levels below roughly 5 km. The lowest level is at roughly 40 metres with four levels typically covering the BL. Typical heights and pressures corresponding to the C-CAM sigma levels are given in Table 2.

In order to ensure good timing agreement of the frontal passages with the sequence of synoptic analysis, the simulations cover a 96-hour period consisting of the observed nucleation event and the time leading up to it. The model was run as a sequence of four independent 24-hour simulations, starting at 0000 UTC. Even a limited time drift would possibly lead to a marked anomaly between the simulated time of the frontal passage and that observed. No special vertical mode or normal mode initialisation was performed in these experiments because it was found to be unnecessary with the well-balanced National Centers for Environmental Prediction (NCEP) analyses.

Figure 5 presents the C-CAM simulated MSLP and the winds at the lowest level for the event of 14 August 2000. These simulations are in reasonably close agreement with the analysis in Fig. 1. The simulation suggests that the front arrived sometime shortly after 0600 UTC, while the observations found the front to occur at 0500 UTC. The wind directions for the 24 hours following the front are from the south-west to west, suggesting baseline conditions. This is consistent with the observations made at CGBAPS. A comparison of the simulated and observed water mixing ratio (rw) and temperature (T) in Fig. 6 shows, in general, good skill given the limited resolution of the C-CAM simulations. These time series all show that following frontal passage, the BL water vapour mixing ratio declines, as suggested earlier. Both observed and modelled temperatures initially decline after the frontal passage; then the modelled temperature change stabilises but the observed temperature increases for a short period around the nanoparticle peak time before it decreases further. The decrease in water vapour mixing ratio is consistent with the entrainment of air from the FT.

Figure 7 shows the back-trajectories for this simulation ending at CGBAPS at 2100 UTC 14 August 2000. The three back-trajectories have final heights of roughly 40, 2000 and 5000 metres (refer to Table 2 to translate between heights and sigmas). These trajectories include a vertical motion calculated using the C-CAM vertical velocity, which is shown at the top plot in Fig. 7. Since the 2000 and 5000 metre back-trajectories are clearly out of the BL, they are likely to better simulate the vertical motion than the 40 metre trajectory. The upper-level trajectories are in the FT and therefore are not influenced by the turbulent mixing

Table 2. Typical heights and pressures corresponding to the C-CAM sigma levels. P and P_s stand for actual and surface pressures respectively.

Level	*Sigma* (P/P_s)	*Typical height (m)*	*Typical pressure (hPa)*
1	0.9955	37.63	995.54
2	0.9784	183.66	978.40
3	0.9458	466.85	945.82
4	0.8999	879.91	899.86
5	0.8426	1419.08	842.59
6	0.7761	2083.67	776.06
7	0.7023	2875.97	702.33
8	0.6235	3801.43	623.46
9	0.5415	4869.18	541.50
10	0.4585	6093.08	458.51
11	0.3765	7493.32	376.54
12	0.2978	9098.98	297.67
13	0.2239	10957.9	223.94
14	0.1574	13207.2	157.41
15	0.1001	16093	100.14
16	0.0542	20011.6	54.18
17	0.0216	25878.1	21.60
18	0.0045	35947.5	4.46

Fig. 5 C-CAM simulated MSLP and winds at the lowest sigma level (about 38 m) for 14 to 15 August 2000; simulation times are 0600, 1200, 1800 and 0000 UTC.

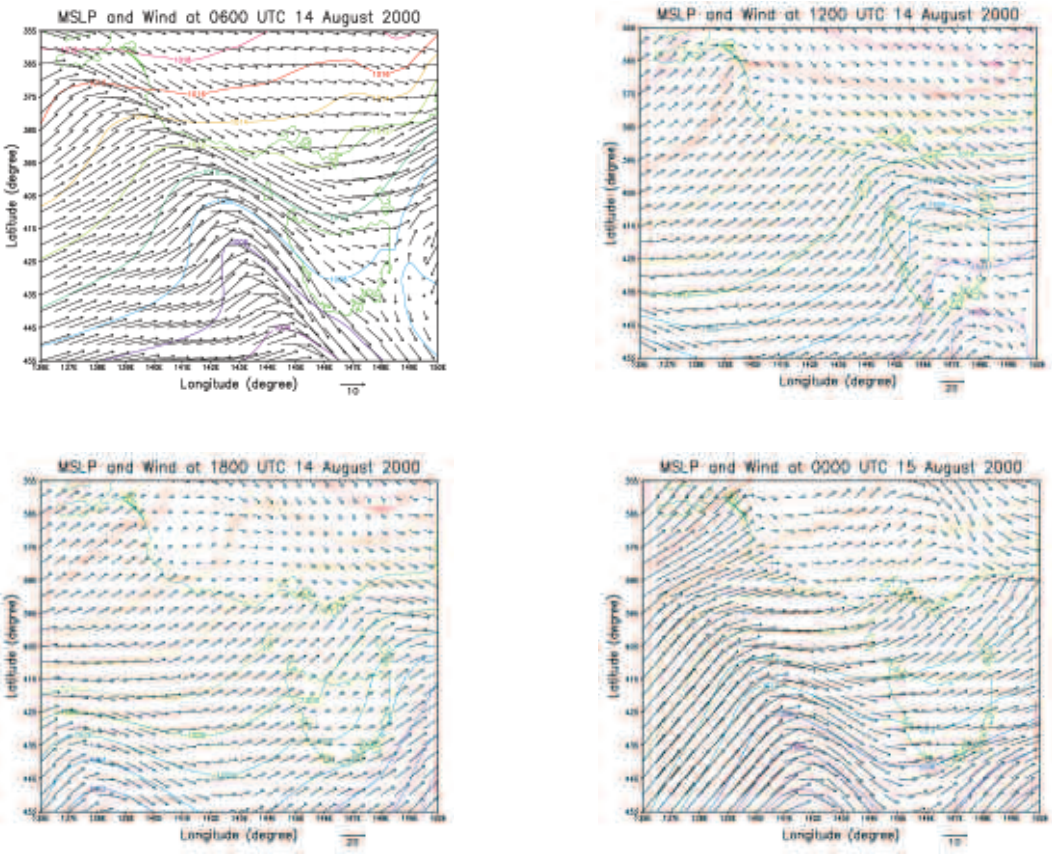

processes occurring in the BL. As the upper trajectories approach CGBAPS, they experience subsidence, which is entirely consistent with the presence of a high pressure ridge and a well defined BL.

As stated earlier, the key insight to be gained from these numerical simulations is the nature of the dynamics of the BL at the time of the observed nucleation events. Ideally, we would like to know whether the BL is entraining overlying air from the FT during these times. Figure 8 (top) presents the BL depth and entrainment rate at CGBAPS from the C-CAM simulation of 14 August. The entrainment rates into the mixed layer were calculated from the model predicted subsidence velocity and growth rate of the mixed layer depth. A peak in the entrainment rate is found at 1500 UTC, which is just before the observed nucleation peak event was observed to start (1700 UTC).

The boundary-layer ozone concentration plot in Fig. 8 (bottom) shows a complex behaviour and there is a less consistent pattern with perhaps a small decrease in ozone during the nanoparticle enhancement. For three of the four examples selected in summer, ozone concentration falls sharply immediately following the passage of a front and almost remains constant during the first 24 hours of the post-frontal period. For the remaining passage in summer, the ozone concentration was a maximum around the time the highest nanoparticle concentration was observed. As in the case of August, the ozone behaviour for the frontal passage in June displayed a rather complex pattern. Although free tropospheric ozone concentration is, on average, greater than at the surface, the FT ozone concentration can be highly variable especially in mid-latitudes where tropopause folds can perturb concentrations.

Table 3 provides details of the C-CAM simulations for the six case studies defined in Table 1. A comparison of the change in temperature and mixing ratio is

Fig. 6 **Observed and C-CAM simulated water mixing ratios (rw) and air temperature (T) for 14 through to mid 16 August 2000. The lowest C-CAM data are plotted as they would be the most closely associated with Cape Grim observations at the surface. The region between blue dashed lines highlights the time of nucleation event.**

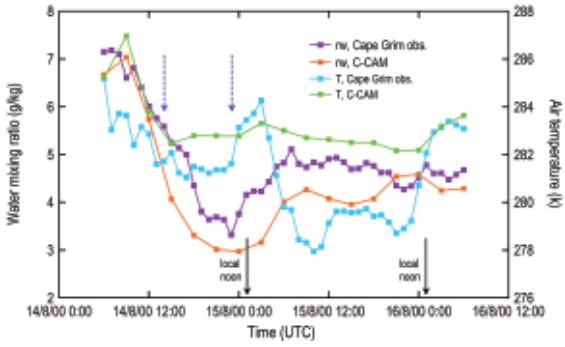

Fig. 7 **96-hour back-trajectories ending at the Cape Grim Baseline Air Pollution Station at elevations of roughly 40 m, 2000 m and 5000 m as defined by the C-CAM simulations of 14 August 2000. The vertical motion for the lowest trajectory in the top figure is obscured because its sigma value is close to one and is overlying on the horizontal axis.**

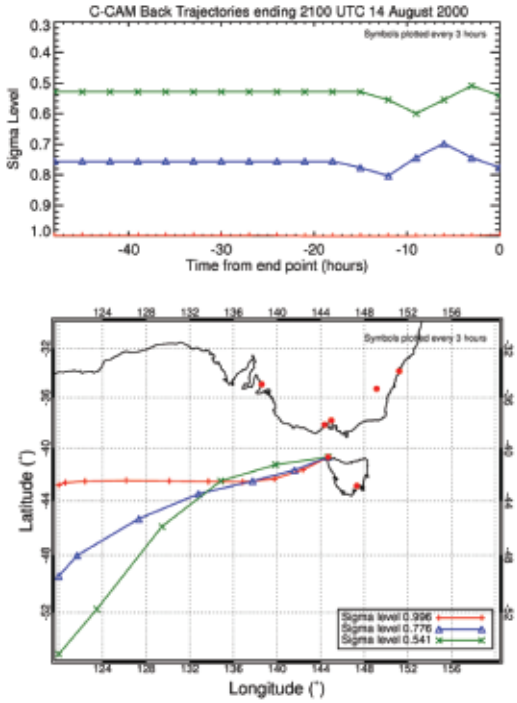

Fig. 8 **C-CAM simulated mixed-layer depth and entrainment rate (top figure), and observed ozone concentration at Cape Grim Baseline Air Pollution Station for 14 through to mid 16 August 2000.**

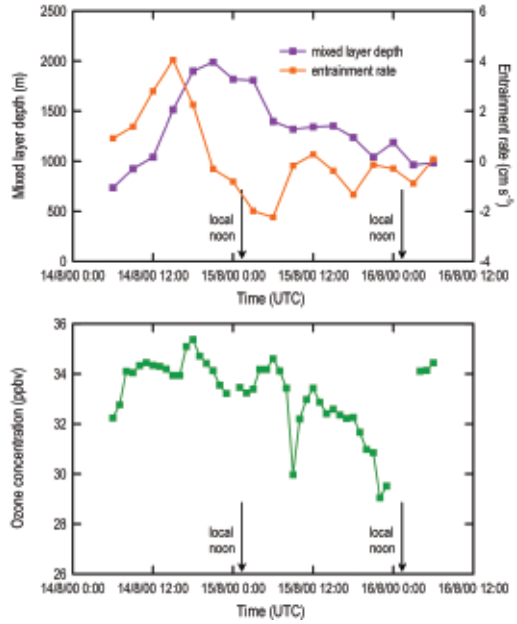

presented, as well as the average entrainment rate from the onset of the nucleation event to its peak. The range of modelled decreases in water vapour mixing ratio was the same as that observed (i.e. 0.6 – 3.7 g kg^{-1}), and the temperature decrease ranged from 0.8 – 4.1 K. Both observed and modelled water mixing ratios are consistent with the characteristics of air that has been entrained from the FT into the BL.

Discussion

It appears implausible that these nanoparticles would nucleate within the BL, due to the presence of pre-existing particles; for example, sulfur species derived from marine dimethylsulfide (DMS) emissions (Cainey and Harvey 2002; Pirjola et al. 2000) would preferentially condense onto pre-existing particles. It would also appear implausible for the nucleation events to be linked to coastal processes as these events have been observed over the remote Southern Ocean, far removed from the coast. O'Dowd et al. (1999) reported significant coastal production linked to halide emission at Mace Head,

Table 3. C-CAM simulations at times of nucleation events.

Time of nucleation event peak (UTC)	*Entrainment rate at onset of event (cm s^{-1})*	*Boundary-layer depth at peak (m)*	*Δ BL water vapour (g kg^{-1})*	*Δ BL temperature (K)*
0300 15 Feb 1999	2.58	1122	10.5-6.8	288.6-287.1
1700 17 Feb 1999	-1.06	496	8.2-5.6	287.7-284.8
2300 03 Jun 2000	0.47	1243	5.6-4.8	285.4-284.3
2300 14 Aug 2000	2.25	1905	7.0-3.4	287.0-282.9
0000 12 Dec 2000	1.37	660	8.9-8.3	289.4-288.7
0000 18 Dec 2000	1.27	509	10.3-8.1	291.1-287.8

Ireland, but a recent study by Cainey et al. (2007) has concluded that iodine emissions from seaweeds are not significant contributors to particle formation at Cape Grim. Capaldo et al. (1999) builds a simple model of new particles that shows nucleation can occur after heavy rain (wet deposition) removes existing particles. Our observations find evidence of nucleation events in periods when there has not been heavy precipitation.

The most plausible explanation for the presence of these nanoparticles is for them to have been created at or above the inversion in the outflow of the shallow cumulus clouds commonly observed in association with the ridging between frontal passages and subsequently entrained into the BL. Numerous studies have shown that significant concentrations of new particles are observed near cloud tops (e.g. Perry and Hobbs 1994; Clarke et al. 1998; Weber et al. 2001).

Jimi (2004) explored the explanation or connection suggested by Bates et al. (1998) that these nucleation events are related to frontal passages, concluding that it was unlikely that the actual frontal passage was directly linked to the following nucleation event; rather that the nucleation event was weakly correlated with the post-frontal BL itself.

Surface observations at CGBAPS verify the skill of the C-CAM simulations for the six case studies. In all cases the modelled BL becomes increasingly dry with time, which is consistent with the entrainment of dry, overlying air from the FT. The C-CAM simulations of the BL also produce a relatively strong entrainment rate in the period of time leading up to the nucleation events. This model of BL nucleation events is physically consistent with the observations of Bates et al. (1998) and Jimi (2004), and is further supported by the conclusions of Raes (1995) on the importance of free tropospheric entrainment in maintaining particle number in the remote subtropical boundary layer.

Conclusion

Nanoparticle observations reported in this study show that whilst frontal passages may precede the conditions that are necessary for post-frontal nanoparticle enhanced events, the front is not the main controlling factor for their characteristics. Simulations of frontal passages using a variable-resolution global climate model predicted vertical motion (descent) of air masses around the time that the maximum enhancement in nanoparticle concentration was observed. Once the particles are entrained into the MBL they become part of the normal boundary-layer mixing process. For the selected examples, the simulations show that the post-frontal enhancement events typically coincide with the deepening of the mixing-layer depth, during which lower FT air is entrained into the growing boundary layer. This period is also marked by maximum drying or a minimum in water vapour mixing ratio, expected with increased entrainment of drier FT air. Satellite images show that low-level cumulus, specifically small, scattered, cellular clouds, are also typical during these periods of enhancement. This provides a plausible source for new particles in the lower FT that can subsequently be entrained into the boundary layer and mixed to the surface.

Acknowledgments

We would like to acknowledge the effort of the staff at the Cape Grim Baseline Air Pollution Station. The authors are also grateful to the Australian Bureau of Meteorology for providing MSLP charts and GMS IR satellite imagery. Raw data for the high resolution NOAA satellite imagery was kindly provided by CSIRO Office of Space Science and Applications Earth Observation Centre. The authors acknowledge helpful suggestions from the reviewers.

References

Bates, T.S., Kapustin, V.N., Quinn, P.K., Covert, D.S., Coffman, D.J., Mari, C., Durkee, P.A., De Bruyn, W.J. and Saltzman, E.S. 1998. Processes controlling the distribution of aerosol particles in the lower marine boundary layer during the First Aerosol Characterisation Experiment (ACE 1). *J. Geophys. Res., 103,* 16 369-83.

Bigg, E.K., Gras, J.L. and Evans, C. 1984. Origin of Aitken particles in remote regions of the Southern Hemisphere. *J. Atmos. Chem., 1,* 203-14.

Boers, R., Ayers, G.P. and Gras, J.L. 1994. Coherence between seasonal variation in satellite-derived cloud optical depth and boundary layer CCN concentrations at a mid-latitude Southern Hemisphere station. *Tellus, 46B*, 123-31.

Cainey, J. and Harvey, M. 2002. Dimethylsulfide, a limited contributor to new particle formation in the clean marine boundary layer. *Geophys. Res. Lett., 29,* 1128-31.

Cainey, J.M., Keywood, M., Grose, M.R., Krummel, P., Galbally, I.E., Johnston, P., Gillett, R.W., Meyer, M., Fraser, P., Steele, P., Harvey, M., Kreher, K., Stein, T., Ibrahim, O., Ristovski, Z.D., Johnson, G., Fletcher, C.A., Bigg, E.K and Gras, J.L. 2007. Precursors to particles (P2P) at Cape Grim 2006: campaign review. *Environ. Chem., 4,* 143-50.

Capaldo, K.P., Kasibhatla, P. and Pandis, S.N. 1999. Is aerosol production within the remote marine boundary layer sufficient to maintain observed concentrations? *J. Geophys. Res., 104*, 3483-500.

Clarke, A.D. 1993. Atmospheric nuclei in the Pacific midtroposphere: their nature, concentration, and evolution. *J. Geophys. Res., 98*, 20 633-47.

Clarke, A.D., Varner, J.L., Eisele, F., Mauldin, R.L., Tanner, D. and Litchy, M. 1998. Particle production in the remote marine atmosphere: Cloud outflow and subsidence during ACE 1. *J. Geophys. Res., 103*, 16 397-409.

Covert, D.S., Kapustin, V.N., Quinn, P.K. and Bates, T.S. 1992. New particle formation in the marine boundary layer. *J. Geophys. Res., 97*, 20 581-9.

Covert, D.S., Kapustin, V.N., Bates, T.S. and Quinn, P.K. 1996. Physical properties of marine boundary layer aerosol particles of the mid-Pacific in relation to sources and meteorological transport. *J. Geophys. Res., 101*, 6919-30.

Hogan, A.W. and Barnard, S. 1978. Seasonal and frontal variation in Antarctic aerosol concentrations. *Jnl appl. Met., 17,* 1458-65.

Ito, T. 1985. Study of background aerosols in the Antarctic troposphere. *J. Atmos. Chem., 3,* 69-91.

Jimi, S.I. 2004. Nanoparticles in the marine boundary layer: a regional perspective using in situ observations at Cape Grim, Tasmania-Australia. Doctor of Philosophy thesis, Monash University, Melbourne, Australia.

McGregor, J.L. 1996. Semi-Lagrangian advection on conformal-cubic grids. *Mon. Weath. Rev., 124*, 1311-22.

McGregor, J.L. and Dix, M.R. 2001. The CSIRO conformal-cubic atmospheric GCM. *Symposium on Advances in Mathematical Modelling of Atmosphere and Ocean Dynamics*, Kluwer Academic Publishers, Netherlands, 197-202.

O' Dowd, C.D., Geever, M., Hill, M.K., Smith, M.H. and Jennings, S.G. 1998. New particle formation: Nucleation rates and spatial scales in the clean marine coastal environment. *Geophys. Res. Lett., 25*, 1661-4.

O'Dowd, C.D., McFiggans, G., Creasey, D.J., Pirjola, L., Hoell, C., Smith, M.H., Allan, B.J., Plane, J.M.C., Heard, D.E., Lee, J.D., Pilling, M.J. and Kulmala, M. 1999. On the photochemical production of new particles in the coastal boundary layer. *Geophys. Res. Lett., 26*, 1707-10.

O'Dowd, C.D., Hameri, K., Makela, J. M., Pirjola, L., Kulmala, M., Jennings, S.G., Berresheim, H., Hansson, H.C., de Leeuw, G. Kunz, G. J., Allen, A.G., Hewitt, C.N., Jackson, A., Viisanen, Y. and Hoffmann, T. 2002. A dedicated study of New Particle Formation and Fate in the Coastal Environment (PARFORCE): overview of objectives and achievements. *J. Geophys. Res., 107*, 8108-23.

Perry, K.D. and Hobbs, P.V. 1994. Further evidence for nucleation in clear air adjacent to marine cumulus clouds. *J. Geophys. Res., 99*, 22 803-18,

Pirjola, L., O'Dowd, C.D., Brooks, I.M. and Kulmala, M. 2000. Can new particle formation occur in the clean marine boundary layer? *J. Geophys. Res., 105*, 26 531-46.

Raes, F. 1995. Entrainment of free tropospheric aerosols as a regulating mechanism for cloud condensation nuclei in the remote marine boundary layer. *J. Geophys. Res., 100,* 2893-903.

Weber, R.J., Chen, G., Davis, D.D., Mauldin, R.L., Tanner, D.J., Eisele, F.L., Clarke, A.D., Thornton, D.C. and Bandy, A.R. 2001. Measurements of enhanced H_2SO_4 and 3-4 nm particles near a frontal cloud during the First Aerosol Characterization Experiment (ACE 1). *J. Geophys. Res., 106*, 24 107-17.